PRAMANA — journal of physics | © Indian Academy of Sciences | Vol. 75, No. 4 October 2010 pp. 639–648

Search for $B_s \to \phi\mu\mu$ decay at the Large Hadron Collider

SUPREET PAL SINGH[1], K MAZUMDAR[2] and J B SINGH[1]
[1]Department of Physics, Panjab University, Chandigarh 160 014, India
[2]Tata Institute of Fundamental Research, Homi Bhabha Road, Navy Nagar, Mumbai 400 005, India
*Corresponding author. E-mail: mazumdar@mailhost.tifr.res.in

MS received 10 September 2009; revised 19 April 2010; accepted 28 April 2010

Abstract. As B_s-mesons will be produced abundantly at the LHC, the observability of the flavour-changing-neutral-current decay mode $B_s \to \phi\mu^+\mu^-$ has been studied in CMS at the LHC centre-of-mass energy of 10 TeV. With an integrated luminosity of 100 pb^{-1}, an upper limit of 6.7×10^{-6} on the branching ratio is expected to be obtained. The potential at 7 TeV with a luminosity of 1 fb^{-1} is expected to be better .

Keywords. B_s-mesons; Large Hadron Collider.

PACS No. 14.40.nd

1. Introduction

The decay $b \to s\ell^+\ell^-$ is a flavour-changing-neutral-current (FCNC) process, where the flavour of the original quark b is changed to a same charged quark s, accompanied by a pair of opposite sign same flavour leptons. Various FCNC processes have led to important understandings in high energy physics during the last several decades. FCNC decays are absent in the Standard Model (SM) at tree level but they proceed at higher order through electroweak penguin and box diagrams. New Physics interactions beyond SM often leave their signatures via quantum corrections manifesting in tiny deviations from standard expectations and hence measurement of the rare decays are always interesting. Only a high luminosity machine can produce sufficient number of mother particles and hence provide opportunities to search for rare decays and thereby the possibility to probe physics of much higher energy scale. The LHC will produce B_s-mesons abundantly at all the centre-of-mass energies being envisaged right now. Thus study of rare decay modes of B_s-meson system will constitute a major physics programme at LHC during the initial years when the scope of direct manifestation of possible New Physics signatures, like production of supersymmetric particle pairs, are limited [1].

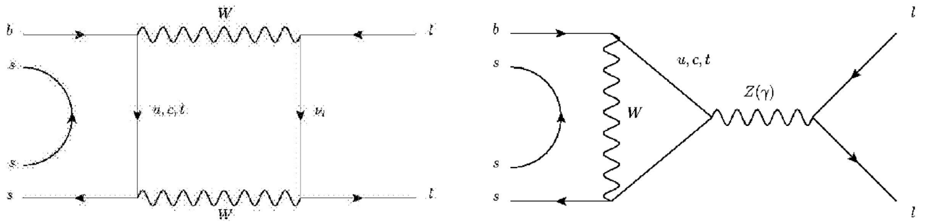

Figure 1. One-loop box and penguin diagrams for the short-distance contribution in the SM.

The inclusive FCNC decays like $B \rightarrow X_s l^+ l^-$ or $B \rightarrow X_s \gamma$ are theoretically easier to calculate, but it is the exclusive decays with one hadron in the final state that are experimentally easier to study. Interestingly, the exclusive decays $B_d \rightarrow K^* l^+ l^-$ and $B^\pm \rightarrow K^\pm l^+ l^-$ have already been measured at B-factories [2,3] and were found to be consistent with the SM within the experimental uncertainties. However, the forward–backward asymmetry, as a function of the square of the dilepton invariant mass, shows significant deviation from the Standard Model which may hint New Physics effect [4]. The same quark-level transition of $b \rightarrow s l^+ l^-$ is effective in the exclusive FCNC decay $B_s \rightarrow \phi \mu^+ \mu^-$ as shown in figure 1. The rate of this process is predicted to be about 1.6×10^{-6} in SM [5]. Hence an observation of this process will yield interesting information on the flavour dynamics of the FCNC decays. This decay has also been searched in Tevatron experiments [6]. The potential of general purpose experiments at the LHC to identify this channel has been estimated using realistic simulation of the signal and the backgrounds, in the context of Compact Muon Solenoid (CMS) detector configuration.

2. Compact Muon Solenoid (CMS) detector

A detailed description of the CMS experiment can be found in [7]. The central feature of the CMS apparatus is a superconducting solenoid, with an internal diameter of 6 m. Within the field volume are the silicon pixel and strip tracker, the crystal electromagnetic calorimeter and the brass-scintillator hadronic calorimeter. Muons are measured in gas chambers embedded in the iron return yoke. Besides the barrel and endcap detectors, CMS has extensive forward calorimetry.

The tracker is designed for the high resolution momentum measurement of charged particles and vertex reconstruction in the pseudorapidity range of $|\eta| < 2.4$ [8]. Mid-rapidity charged particles are tracked by three layers of silicon pixel detectors, made of 66 million 100×150 μm^2 pixels, followed by ten microstrip layers, with strips of pitch-size between 80 and 180 μm. The silicon tracker provides the vertex position with about 15 μm accuracy.

The muons are measured using three types of detection technologies: Drift tubes, cathode strip chambers, and resistive plate chambers. Matching the muons to the tracks measured in the silicon tracker results in a transverse momentum resolution between 1 and 5%, for transverse momentum values up to several TeV/c.

3. Simulation of signal and background events

The production of bottom–antibottom quark pairs at the LHC as well as the main background process of hadronic events both arise due to strong interactions via the gluon–gluon fusion, the flavour excitation and the gluon splitting modes involving quarks and gluons in the initial state. The signal process of $B_s \to \phi\mu^+\mu^-$ is one of the weak decays of B_s-meson which is produced during hadronization of the bottom quark. The charge-conjugate process is always implied and taken into account in this study. We refer the background events simply as QCD here. These generic QCD 2→2 partonic subprocesses are produced using PYTHIA Monte Carlo generator package [9] and the structure functions determined according to CTEQ5L parametrization. The total hadronic cross-section at the centre-of-mass energy of 10 TeV is taken to be 51.6 mb though this value has very large theoretical uncertainty, mostly due to parton density function.

For discriminating the signal process from the plethora of hadronic interactions as explained above, the event is first required to contain at least one b-quark which then hadronizes to a B_s-meson with 10% probability. Subsequently the B_s-meson is decayed to the $\mu\mu\phi$ mode through a specially dedicated B-meson Monte Carlo generator package, EvtGen [10]. The final mode is studied when $\phi \to K^+K^-$ with 50% branching ratio. The generator level filter efficiency for the signal events is 2.1×10^{-2}%.

In proton–proton collision at the LHC, a large number of events will involve only low-energy particles and hence they are not particularly interesting other than dedicated study of minimum-bias events. Hence on-line trigger conditions are applied based on the transverse momenta of final-state particles to select and record events involving energetic particles. Thus, while preparing the analysis strategy for optimum use of the computer resources during simulation, an event-filter based on the kinematic properties of the generated daughter particles has been applied. Each event is required to have at least two muons with minimum transverse momentum $P_{\mathrm{T}} \geq 2.5$ GeV/c and pseudorapidity of $|\eta| < 2.4$. These kinematic conditions yield an acceptance of about 12% only for signal events.

These generated events are finally simulated through the detector configuration of CMS experiment using GEANT4 package to emulate various detector effects. Almost 9K fully simulated signal events have been studied which correspond to an integrated luminosity of 1 fb^{-1}. Similarly, a total of about 5 million QCD background events were studied which were selected demanding the presence of at least one muon with a transverse momentum of $P_{\mathrm{T}} \geq 2.5$ GeV/c and pseudorapidity of $|\eta| < 2.4$ at the level of event generation. Since the selection of events having two muons are preceeded by the reconstruction of the events after simulation in the detector, any possibility of misidentification of the jet as a muon is accounted for. However, the jet-faking probability is relatively low and mostly the second muon in the background event may have various sources including heavy meson decays. The background event-statistics correspond to an integrated luminosity of 0.04 pb^{-1} only. The result presented here corresponds to signal and background events, each of which separately (and collectively as well) are distributed according to Poisson statistics, though the event content of each bin in any distribution is binomial. It is to be noted that the background due to misidentification of hadrons is not accounted for separately, as the probability is very less, about 10^{-5}. In actual experiment, data-driven methods have to be applied to account for such effects.

4. Selection of events

During the actual data taking, the events are considered worthy for further studies if they inclusively contain two muons, of opposite electrical charges and each having a transverse momentum above 3 GeV/c and $|\eta| < 2.4$. The effect of this event trigger condition is implemented along with off-line selections during the present analysis with fully reconstructed and calibrated objects. As CMS detector does not have particle identification capabilities, the analysis starts with identifying charged tracks compatible with kaons originating from ϕ-decay mass.

In the event containing a B_s-meson, the probability of a hadronic jet opposite to the direction of flight of the B_s is high. Therefore, the kaons from B_s decay are expected to be produced in the opposite hemisphere with respect to the leading jet in the event. From the collection of all reconstructed tracks in the event, only the subset of the tracks with transverse momentum $P_{\mathrm{T}} \geq 400$ MeV/c and $|\eta| \leq 2.4$ are selected which traverse in the direction opposite to the leading jet, i.e., $\eta^{\mathrm{jet}} \times \eta^{\mathrm{track}} \leq 0$, where η^{jet} and η^{track} are the pseudorapidities of the leading jet and the track respectively. Assigning kaon mass to each of these tracks, invariant mass is constructed from track pairs of opposite charge combination. The candidate kaons correspond to the pair with mass closest to ϕ-meson (1.02 GeV/c^2) within a 3σ window of 1.005 GeV/c^2 $\leq M_{K^+K^-} \leq$ 1.035 GeV/c^2.

In the next step, the invariant mass distribution of $\mu^+\mu^-K^+K^-$ is constructed as shown in figure 2. The dominance of the background, by several orders of magnitude over the signal, may be appreciated from figure 3a. Subsequently, the events are selected where the combined mass of muon and kaon pairs lie around B_s mass region, i.e., 4.5 GeV/c^2 $\leq M_{\mu^+\mu^-K^+K^-} \leq$ 6.3 GeV/c^2. The peak in the mass distribution from the signal sample is fitted with Gaussian function whose mean and rms values are 5.368 and 0.041 GeV/c^2 respectively. The signal event candidates are selected within 3σ around the mean value, i.e., 5.245 GeV/c^2 $\leq M_{\mu^+\mu^-K^+K^-} \leq$ 5.491 GeV/c^2.

Having selected the tracks which presumably correspond to the kaons from B_s decay, the events are now required to pass through a set of preliminary selection criteria based on only the muon pairs in the event.

Invariant mass distribution for the dimuon pair for the range of our interest is plotted in figure 3b. The events are selected in the range 1.4 GeV/c^2 $\leq M_{\mu\mu} \leq$ 4.4 GeV/c^2. Further, to reduce the peaking backgrounds from J/ψ and $\Psi(2S)$ resonances, centred around 3.10 GeV/c^2 and 3.68 GeV/c^2 respectively, a double mass veto is applied around 3σ range of masses for these two. Thus, events are rejected if the dimuon mass falls in the range 2.95 GeV/c^2 $\leq M_{\mu^+\mu^-} \leq$ 3.25 GeV/c^2 or 3.59 GeV/c^2 $\leq M_{\mu^+\mu^-} \leq$ 3.77 GeV/c^2, respectively.

To calculate the number of background events in the signal region, the QCD background spectrum as shown in figure 4a, is fitted with an exponential function of the type $f(x) = \exp(y_0 + y_1 \times x)$ where x is the invariant mass $M_{\mu^+\mu^-K^+K^-}$, y_0 and y_1 are constants which are determined to be $y_0 = 0.754 \pm 0.081$ and $y_1 = 0.174$

± 0.015. The ratio of events in the signal region (5.245 GeV/c^2 to 5.491 GeV/c^2) to that in the sideband regions on both sides, is calculated using the above curve as

$$\text{Integral fraction } (\epsilon_{\rm I}) = \frac{N_{\rm events} \text{ in the signal region}}{N_{\rm events} \text{ in the sidebands}}.$$

About 0.132 fraction of the total QCD events fall under the signal region.

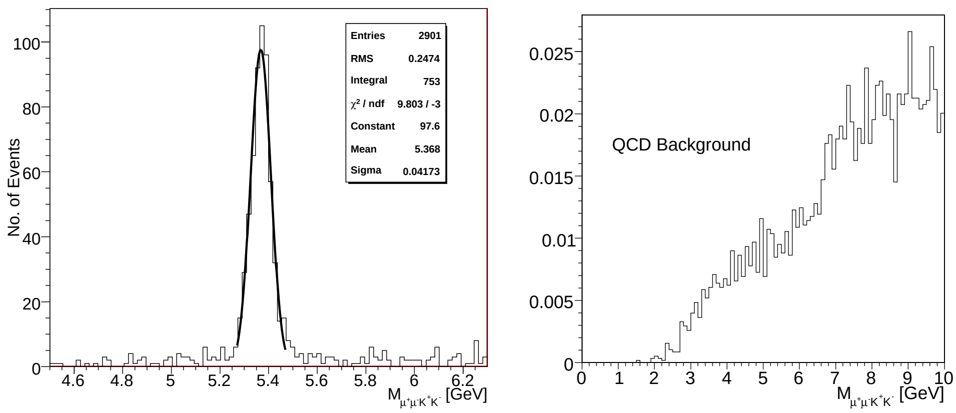

Figure 2. Invariant mass distribution of $\mu^+\mu^-K^+K^-$ after trigger and candidate selection for the signal and the QCD background. The events in the mass window 4.5 GeV/c^2 $\leq M_{\mu^+\mu^-K^+K^-} \leq$ 6.3 GeV/c^2 are considered for further analysis.

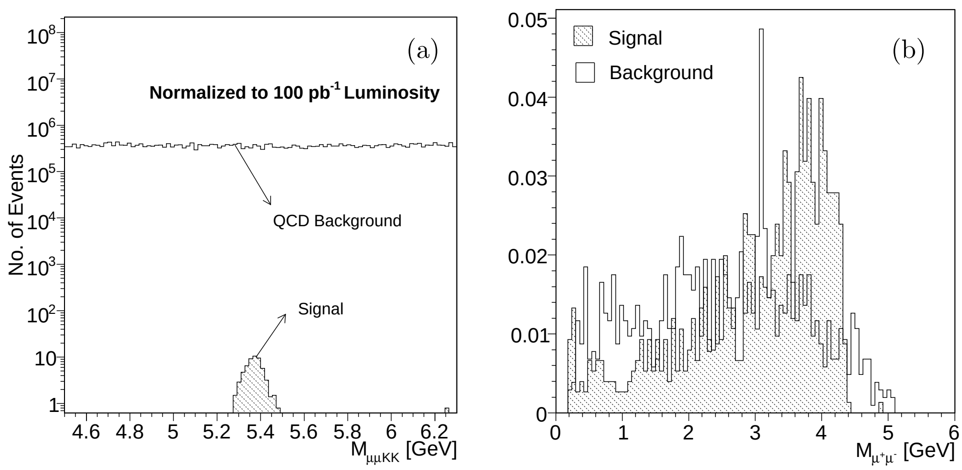

Figure 3. (**a**) B_s peak from signal events compared with QCD background in the invariant mass distribution of $\mu^+\mu^-K^+K^-$ combination and (**b**) invariant mass of the dimuon pair for signal and background distribution after candidate selection. The histograms are normalized to unity.

Table 1. The relative efficiency at each step of the event selection upto preliminary cuts, for signal and QCD background events.

Selection criteria	Eff. for $B_s \to \phi\mu\mu$	Eff. for QCD background
Trigger ($P_{\rm T}^{\mu} \geq 3$ GeV/c and $\lvert\eta^{\mu}\rvert \leq 2.4$)	0.489	0.006
Candidate selection for B_s^0s	0.684	0.731
Events in side bands (including signal region)	0.259	0.047
1.4 GeV/c^2 $\leq M_{\mu\mu} \leq$ 4.4 GeV/c^2 (excluding $J/\psi(1S)$ and $\Psi(2S)$ resonances)	0.660	0.534

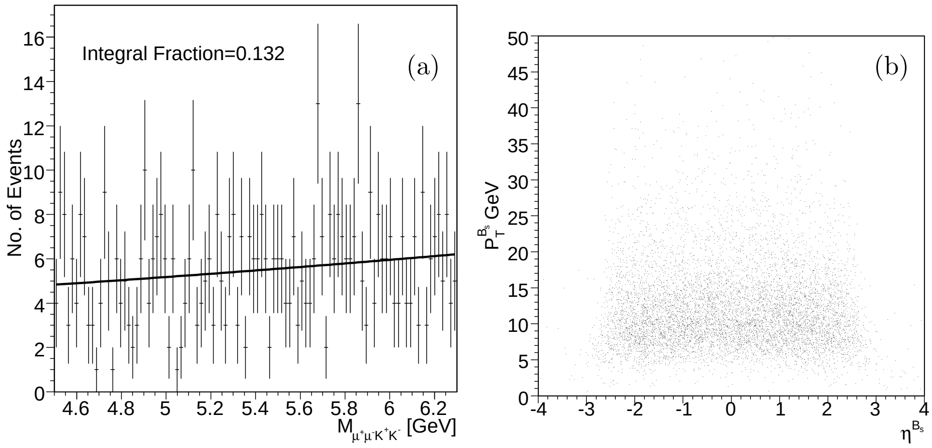

Figure 4. (**a**) Invariant mass distribution of $\mu^+\mu^-K^+K^-$ fitted with an exponential function for QCD background after preliminary cuts and (**b**) generator level $P_{\rm T}$ vs. η plot for the B_s-meson.

The relative selection efficiency values of each criterion for the signal and background samples upto preliminary cuts are given in table 1.

Starting with a total of 8665 simulated signal events, 513 events survive the above preliminary cuts, out of which 391 events fall directly under the signal region. This can be compared with 549 background events remaining in the sample, out of which 487 fall in the sidebands excluding signal region starting with 4663731 number of simulated background events. To reduce the bias of double counting of peaking backgrounds, only events in the sideband regions are further studied and it is required to pass some more criteria to estimate the total number of background events after all cuts.

The transverse momentum of the generated B_s is displayed as a function of its pseudorapidity in figure 4b. The transverse momentum of the reconstructed B_s candidate, calculated from the measured momenta of the dimuons and the kaons, is required to be $P_{\rm T}^{B_s} \geq 11$ GeV/c. The efficiency for this selection is subsequently referred to as ϵ_A.

Thus, in the selected events the B_s-meson is expected to be produced with reasonable boost and hence the daughter particles should not be far from each other. The

Table 2. The relative efficiency at each step of event selection, for signal and QCD background events.

Selection criteria	$B_s \to \phi\mu\mu$ efficiency	QCD Background efficiency
No. of events after preliminary cuts	513	487
$P_{\mathrm{T}}^{B_s} \geq 11$ GeV/c (ϵ_A)	0.665	0.227
$\Delta R_{\mu\mu,\phi} \leq 0.4$ (ϵ_B)	0.371	0.121
$I \geq 0.78$ (ϵ_C)	0.306	0.158
$l_{xy} \geq 0.1$ and $\chi^2 \leq 2$ (ϵ_D)	0.271	0.006

distance in η–ϕ space is computed between dimuon and ϕ system and a maximum threshold of $\Delta R_{\mu\mu,\phi} = \sqrt{\Delta\eta^2 + \Delta\phi^2} \leq 0.4$ is required to be satisfied. Here $\Delta\eta$ and $\delta\phi$ refer to the concerned variables of the dimuon system and the ϕ-candidate. The corresponding efficiency is referred to as ϵ_B.

It is anticipated that there will be more particles around the fake B_s candidate in the QCD background events than around the B_s candidate in the signal events. This feature can be exploited by applying an isolation criterion which is determined from the transverse momentum of the B_s and all the charged tracks around the B_s with $P_{\mathrm{T}} \geq 0.9$ GeV/c, falling within a cone radius of 1.0 in η–ϕ space. This isolation variable is defined as

$$I = \frac{P_{\mathrm{T}}^{B_s}}{(P_{\mathrm{T}}^{B_s} + \Sigma_{\mathrm{trk}} P_{\mathrm{T}})}.$$

A reasonably hard cut of $I \geq 0.78$ is applied for the event selection. The relative efficiency is referred to as ϵ_C.

As the B_s-meson has a finite life-time, it traverses a finite, measurable distance within the detector before decaying. Thus, tracks corresponding to the muons and the kaons are required to originate from a displaced vertex compared to the nominal collsion vertex. The characteristic variables associated with this vertex provide good handles against the combinatoric background. The flight length of the B_s candidate, l_{xy} and the normalized χ^2 for the four track vertex are required to satisfy $l_{xy} \geq 0.1$ and normalized $\chi^2 \leq 2$. The corresponding relative efficiency is referred to as ϵ_D.

The relative efficiency for each criterion after preliminary cuts for the signal and background samples is provided in table 2. All the selection criteria discussed above, viz., the transverse momentum of the reconstructed B_s candidate, distance between daughter particles, track isolation and displaced vertex parameters are uncorrelated to invariant mass of $\mu^+\mu^-K^+K^-$ system. Therefore, the total effect of these selections is taken as the product of all the individual efficiencies.

5. Expected number of signal and background events after selection

The number of signal events surviving in the mass window (5.245, 5.491 GeV/c^2) is

$$N_{\rm sig} = N_s \times \epsilon_A \times \epsilon_B \times \epsilon_C \times \epsilon_D = 7.95,$$

where N_s is the number of events in the signal mass region after preliminary cuts and $\epsilon_A, \epsilon_B, \epsilon_C, \epsilon_D$ are the respective efficiencies for the signal events given in table 2.

The total signal efficiency ϵ_s, considered for the whole mass range can be calculated from the total number of signal events analysed, $N_{\rm tot} = 8665$.

$$\epsilon_s = \frac{N_{\rm sig}}{N_{\rm tot}} = 9.2 \times 10^{-4}.$$

Now the selected signal events of eight signal events correspond to an integrated luminosity of 1000 pb^{-1} which has to be scaled down by a factor of 10, to get the expected number of events at a luminosity of 100 pb^{-1}. Thus, the total number of signal events passing the selection criteria for 100 pb^{-1}, is estimated to be $0.795 \leq 1$ only which is statistically too insignificant.

The number of QCD background events left in the signal region after applying all the factorizing selections can be determined as

$$N_{\rm bkg} = N_{\rm bg} \times \epsilon_A \times \epsilon_B \times \epsilon_C \times \epsilon_D \times \epsilon_I = 0.0019,$$

where $N_{\rm bg}$ is the number of events left in the sidebands and signal region after preliminary cuts which is 549 and $\epsilon_A, \epsilon_B, \epsilon_C, \epsilon_D, \epsilon_I$ are the respective efficiencies for QCD background as given in table 2.

This corresponds to an integrated luminosity of 0.04 pb^{-1} which needs to be scaled up by a factor of 2500 so that the final number corresponds to an integrated luminosity of 100 pb^{-1}. Therefore, the expected total number of QCD events in the signal mass region after all the cuts for 100 pb^{-1}, is estimated to be 4.75.

At present, the LHC is foreseen to deliver proton-on-proton collision at 7 TeV for a considerable length of time, accumulating a luminosity of 1 fb^{-1} per experiment. Considering the reduced centre of mass energy compared to 10 TeV, the kinematics of final-state particles are expected to be softer. This will affect the event acceptance within the detector fiducial. At the same time the production rates of both signal and background events are affected; unfortunately, the reduction in signal being much more due to the reduced gluon density at lower energy. As a fresh simulation at 7 TeV is beyond the scope of this work, we can optimistically estimate the situation assuming same efficiencies for generation, reconstruction and selection of signal and background processes. Thus, at 7 TeV with 1 fb^{-1} of integrated luminosity, the number of signal and background events expected to be selected are 7.48 and 46.4. These numbers are almost 10 times larger when compared with the event yields at 10 TeV with 100 pb^{-1}. Thus, the signal significance will be three times better at the lower energy of 7 TeV, but for 10 times higher luminosity.

6. Estimation of branching ratio

Evidently, it is impossible to observe any signal above background in data corresponding to a luminosity of 100 pb^{-1}. However, the upper limit on the branching fraction of this decay can be determined by absolute normalization technique by first calculating the upper limit on the number of signal events ($N_{\rm UL}$) which can be observed in the same data. This is obtained from Poisson distribution where the mean value is given by the sum of the expected number of signal and background events as determined above. At 90% confidence level (CL), $N_{\rm UL} = 4.94$.

The 90% CL upper limit on the branching fraction is given by

$$B_{\rm UL} = \frac{N_{\rm UL}}{\epsilon_s \times \epsilon_{\rm gen} \times N_{B_s}},$$

where ϵ_s, the total signal efficiency of the complete analysis chain $= 9.2 \times 10^{-4}$, $\epsilon_{\rm gen}$, the efficiency of kinematic selections applied on daughter particles during event generation = 0.13 and N_{B_s} the expected number of the produced B_s events $=\sigma_{b\bar{b}} \times \mathcal{L} \times f \times 2$ where $\mathcal{L} = 100$ pb^{-1} and $\sigma_{b\bar{b}}$ the $b\bar{b}$ production cross-section = 440 μb at the LHC cm energy of 10 TeV and f is the probability of a b or $\bar{b}$ to hadronize to a B_s-meson = 0.1 and hence a factor of 2 in the calculation. Thus N_{B_s} $= 8.8 \times 10^9$ and therefore at 90% CL, the upper limit on the branching fraction of $\mathcal{B}$ $(B_s \to \phi\mu^+\mu^-)$ is

$$B_{\rm UL} = 6.7 \times 10^{-6}$$

which is more than four times that of the expectation from SM. Hence higher value of accumulated luminosity is needed to study this channel. As the number of events are too small, systematic uncertainties on the result have not been evaluated at this stage.

As discussed above, the signal significance being much better at the LHC energy of 7 TeV and integrated luminosity of 1 fb^{-1}, a better limit on the branching ratio is anticipated. With larger number of events, several measurements can be performed including angular distribution and forward–backward asymmetry. More importantly while searching for new physics, the signal yield can be normalized with respect to the well-measured channel of $J/\psi \to \mu^+\mu^-$ to reduce various systematics.

7. Summary

A cut-based analysis procedure has been established to observe the process $B_s \to \phi\mu^+\mu^-$ during the early phase of the LHC at the centre-of-mass energy of 10 TeV. With 100 pb^{-1} of accumulated luminosity in CMS detector, the signal is not observable. However, an upper limit on the branching fraction of the decay $\mathcal{B}(B_s \to \phi\mu^+\mu^-) \leq 6.7 \times 10^{-6}$ is expected to be obtained.

Acknowledgements

The authors sincerely thank R Covarelli for his help and guidance in using EvtGen for the generation of signal samples and S Dasu for providing resources at University of Wisconsin CMS-Tier2-Grid to simulate signal samples.

References

[1] G Buchalla *et al*, arXiv:0801.1833v1 [hep-ph]
[2] BaBar Collaboration: B Aubert *et al*, arXiv:hep-ex/0507005
[3] Belle Collaboration: A Ishikawa *et al*, *Phys. Rev. Lett.* **91**, 261601 (2003)

[4] Belle Collaboration: J T Wei *et al*, *Phys. Rev. Lett.* **103**, 171801 (2009)
[5] C Q Geng and C C Liu, *J. Phys.* **G29**, 1103 (2003)
[6] CDF Collaboration: T Aaltonen *et al*, arXiv:hep-ex/0804.3908
[7] CMS Collaboration: *The CMS experiment at CERN LHC*, *J. Instrum.* **0803**, S08004 (2008)
[8] CMS Collaboration: *CMS detector performance and software*, Physics technical design report, Volume I, CERN/LHCC 2006-001
[9] T Sjostrand, S Mrenna and P Skand, *J. High Energy Phys.* **05**, 026 (2006)
[10] A Ryd, D Lange, N Kuznetsova, S Versille, M Rotondo, D Kirkby, F Wuerthwein and A Ishikawa, *EvtGen A Monte Carlo generator for B-Physics*, BAD 522 V6 EvtGen V00-11-06